Shallow geothermal potential of the northern community of Whapmagoostui-Kuujjuarapik

Rapport de recherche R1927

Félix-Antoine Comeau
Nicolò Giordano
Jasmin Raymond

Institut national de la recherche scientifique
Centre Eau Terre Environnement
April 24, 2020

ISBN : 978-2-89146-946-3 (version électronique)

Dépôt légal - Bibliothèque et Archives nationales du Québec, 2021
Dépôt légal - Bibliothèque et Archives Canada, 2021

OVERVIEW

Remote northern communities in the Province of Québec currently rely on fossil fuels to produce both electricity and heat. Environmental, social and financial costs can be reduced by the deployment of clean and renewable solutions, such as geothermal technologies, whose reliability has already been demonstrated down south. A profound change toward such a new source of energy in the North requires to better understand the thermal state and properties of the underground in remote communities, where data are barely available.

CIMA+, which is a Canadian engineering firm with long-lasting experience in different markets, proposed to tackle this problem looking at low enthalpy geothermal technologies to cover space heating and domestic hot water need of northern buildings. Given its strong presence in the North, with services provided to a number of aboriginal peoples in Ontario and Québec, such as Cree and Inuit, a partnership was started with the Institut national de la recherche scientifique (INRS). The team of Professor Jasmin Raymond has been working to demonstrate the viability of ground-source heat pumps (GSHP) and underground thermal energy storage (UTES) in Nunavik for the last three years.

Hence, the goals of the project are:

1) to evaluate the amount of heat that can be sustainably extracted from the ground below the northern village of Whapmagoostui-Kuujjuarapik by means of GSHP;
2) the volume of energy that can be stored with UTES systems for later use and the efficiency of the whole plant (thermal recovery).

The recently developed G.POT method and a novel approach STOREmap were used to achieve these objectives and ensure that cutting-edge geothermal energy tools will be provided to CIMA+ as a successful result of the partnership.

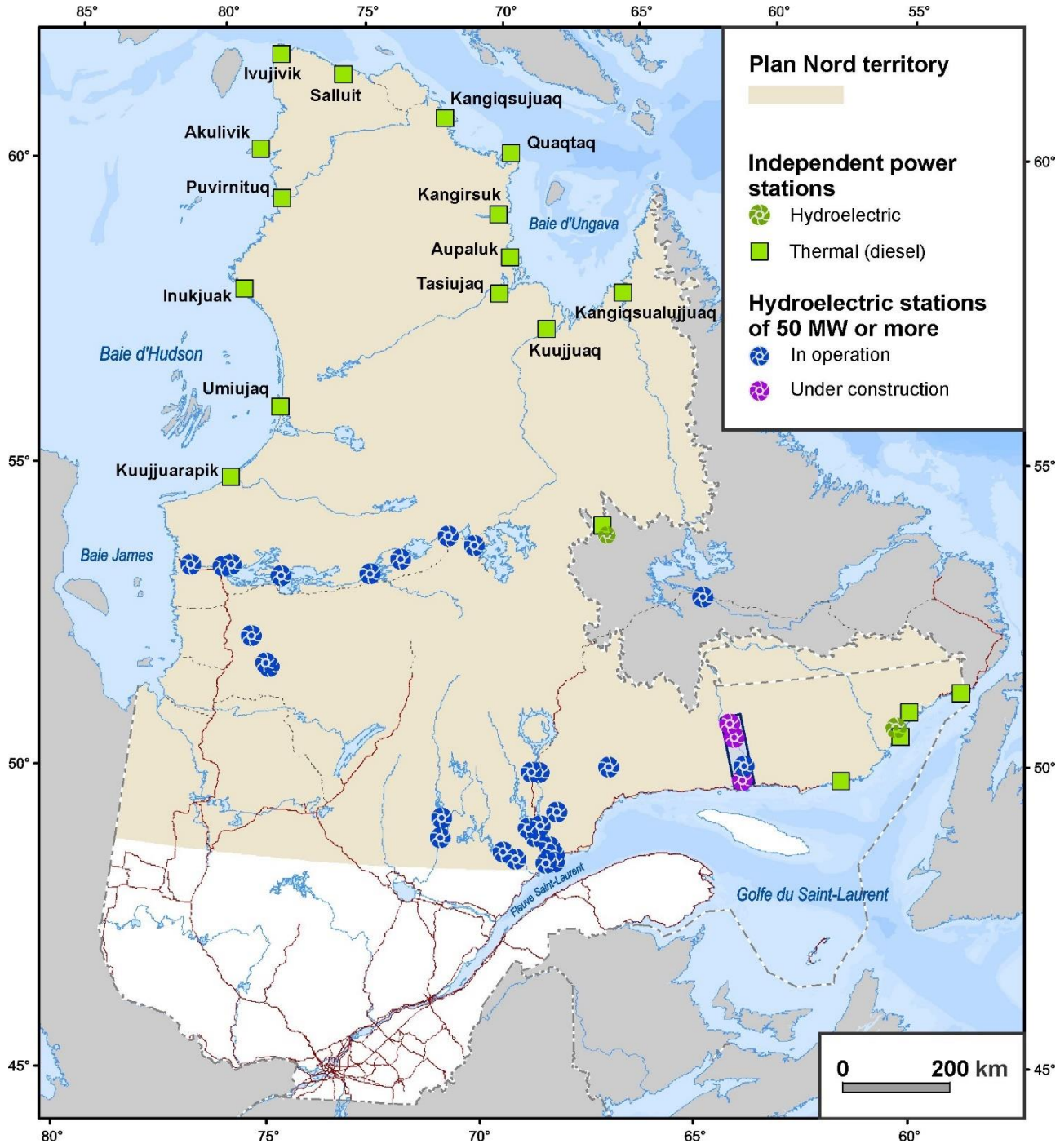

GENERAL CONTEXT

Nunavik is the Inuit territory of the Province of Québec standing north of the 55th parallel, where 14 communities rely on fossil fuels (power plants and furnaces) to produce both electricity and heat (Figure 1). Moreover, with a population of 12 300, Nunavik has a population growth rate of 40 % since 2000 (SHQ, 2014).

Low enthalpy geothermal energy can offer a viable alternative to cover both space heating (SH) and domestic hot water (DHW) demand for northern buildings, but systems would have to be designed according to local conditions. The village of Whapmagoostui-Kuujjuarapik, home to 900 Cree and 650 Inuit people, has been chosen to carry out this project because both partners have experience in the area and important knowledge-base information.

Figure 1 – Electricity generation in the area covered by the Plan Nord (modified from Société du Plan Nord).

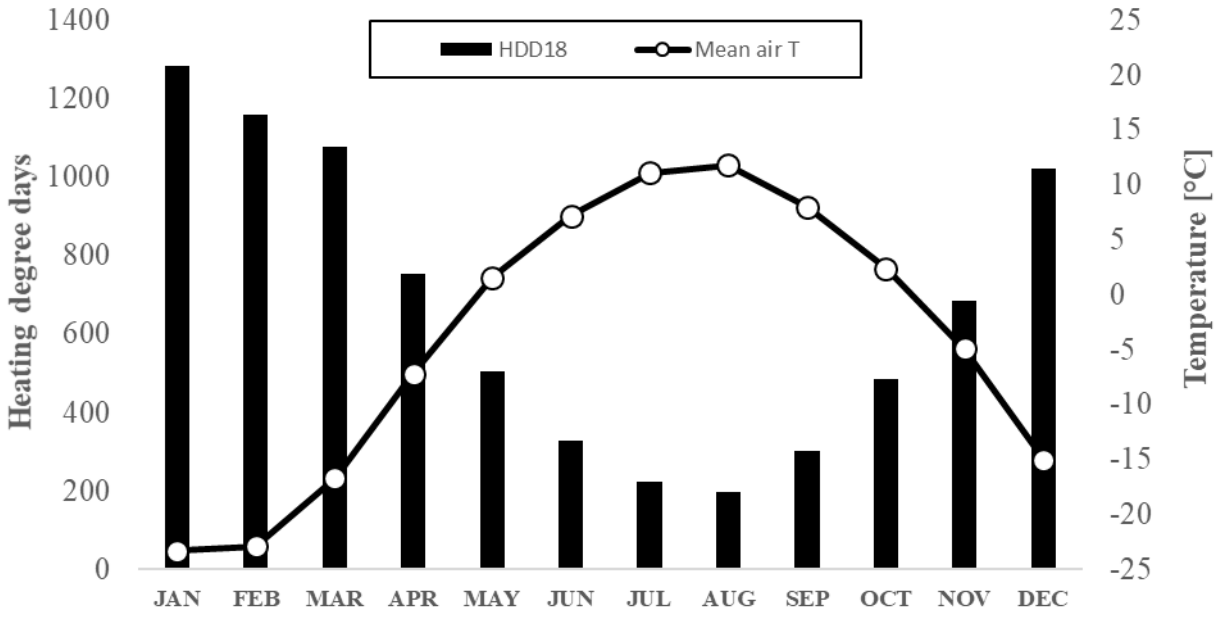

Figure 2 – **Monthly heating degree days below 18 °C and air temperature in Whapmagoostui-Kuujjuarapik.**

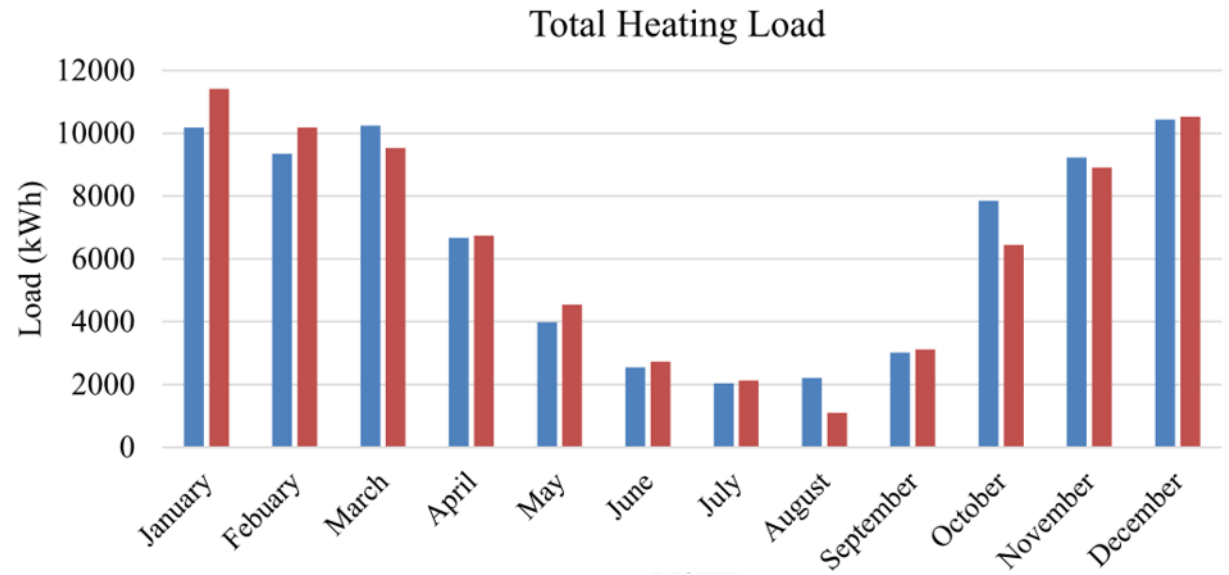

Figure 3 – **Space heating and domestic hot water needs for the reference building in Kuujjuaq (blue bars). Results of a building's energy simulation run with SIMEB (www.simeb.ca/) and calibrated with the US Office of Energy Efficiency and Renewable Energy website (red bars).**

ENERGY DEMAND FOR NORTHERN BUILDINGS

The average air temperature in Whapmagoostui-Kuujjuarapik (W-K) is -4 °C, with a monthly minimum of -23.3 °C in January and monthly maximum of 11.8 °C in August (Figure 2). A clear and simple way to represent the heating needs of a certain place is the heating degree days (HDD). This is the difference between a reference temperature where heating systems start to be operated, usually 18 °C, and the average daily temperature. The sum of this amount for every day of the year gives the annual result. The HDD_{18} in W-K is 8000, while in Québec City is 5100.

Total annual heating loads (space heating and domestic hot water) for a residential building in Kuujjuaq is 71 MWh (mean annual temperature -5.4 °C, HDD_{18} 8500, Figure 3, Gunawan et al., 2020). A building of the research station of the Centre d'études nordiques (CEN) in Kangiqsualujjuaq (mean annual temperature -6 °C, HDD_{18} 8430, Belzile et al., 2017) consumes 68 MWh y^{-1}. We therefore assume a total heating load of 70 MWh y^{-1} for a reference building (150 m^2) in Whapmagoostui-Kuujjuarapik.

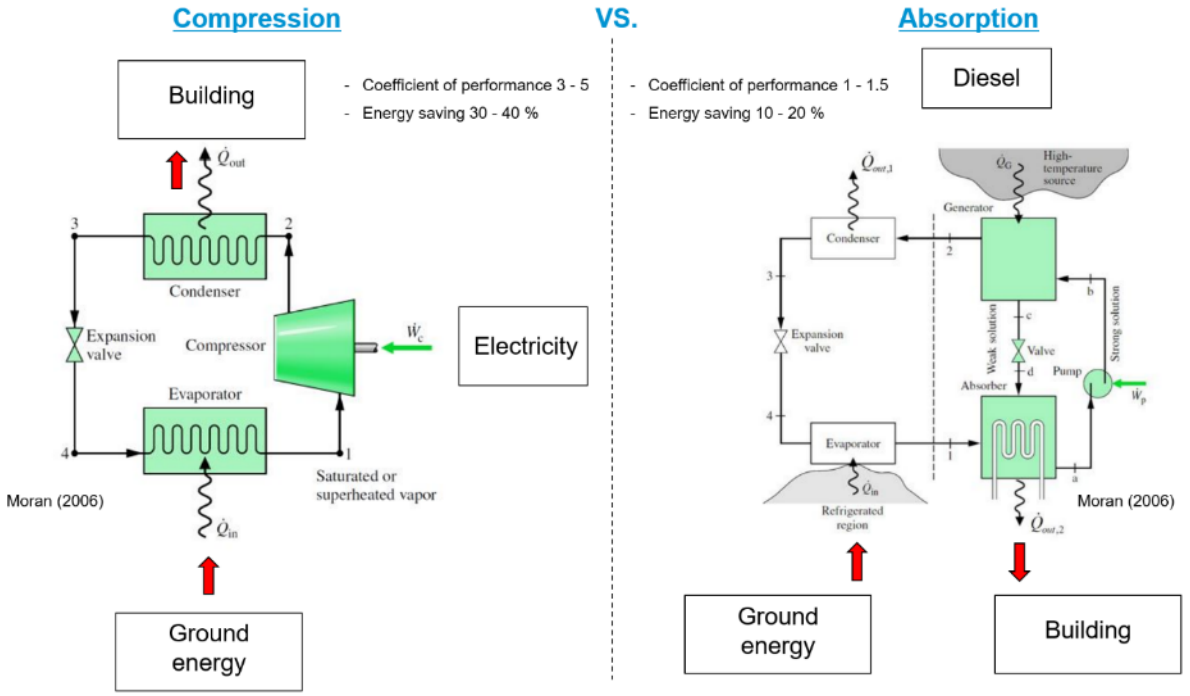

Figure 4 – Basic working principle of a heat pump and difference between those fed by electricity (compression HP, left) and by a heat source such as natural gas or diesel (absorption HP, right; modified from Moran et al., 2018).

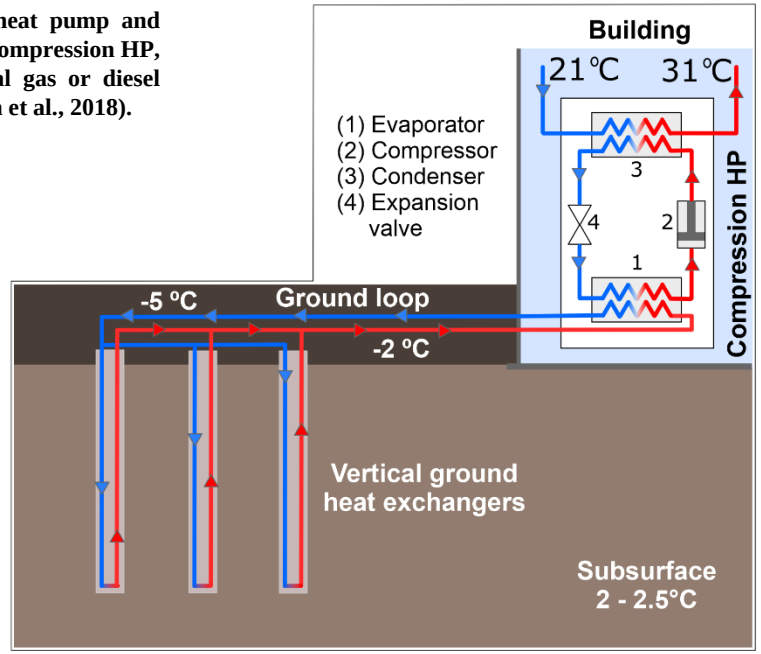

Figure 5 – Diagram of a ground-source HP (compression technology) with 3 GHE (modified from Raymond, 2018). The indicated temperatures represent the context in Whapmagoostui-Kuujjuarapik, where a building can be heated even from a subsurface at 2 °C.

GROUND-SOURCE HEAT PUMPS (GSHP)

A heat pump (HP) is a mature technology that can transfer heat from a « cold source » (air, surface water or underground) to a « warm sink » (the building to be heated) and produces more energy than the work it does. The HP has 4 main elements: evaporator, compressor, condenser and expansion valve. The cold source transfers heat to the evaporator where a low-boiling refrigerant evaporates. The gas is then compressed to increase its temperature, before it gives up the generated heat to the warm sink in the condenser. The expansion valve finally returns the refrigerant at the initial pressure in order to restart the cycle. Two main HP types exist: a compression HP, which needs electricity to run the compressor; an absorption HP, which needs heat (e.g., natural gas, diesel) to run a thermal compressor (Figure 4). Both of them can provide coefficient of performance (COP) bigger than 1, but the compression technology is more efficient. Indeed, for each kW of electricity consumed by the compressor, 3 to 5 kW of heat is transferred to the building (COP = 3 - 5). An absorption HP can offer COP from 1 to 1.5, that is still more than the efficiency of a diesel furnace (0.8) currently used in W-K and the other northern villages.

Ground-source heat pumps (GSHP) have the advantage that the temperature of the cold source, the underground, has a constant temperature over the year due to the thermal inertia of the subsurface. In order to extract the heat from the subsurface, a few drilling wells are necessary to install U-shaped pipes. This installation is commonly known as vertical ground heat exchanger (GHE) and can reach a depth between 100 and 200 m. The current technical temperature limit of the heat pumps is -10 °C. This means that a mixture water/antifreeze (e.g., 25 % of propylene glycol) is able to extract heat from a medium at a temperature as low as 0 °C. As we will show later in the report, the subsurface temperature in W-K in the shallowest 100 m is 2.0 - 2.5 °C. If the ground-loop inlet temperature is -5 °C, we can anticipate a gain of around 3 °C, and the inlet fluid temperature at the evaporator will be -2 °C (Figure 5), enough to properly run the HP.

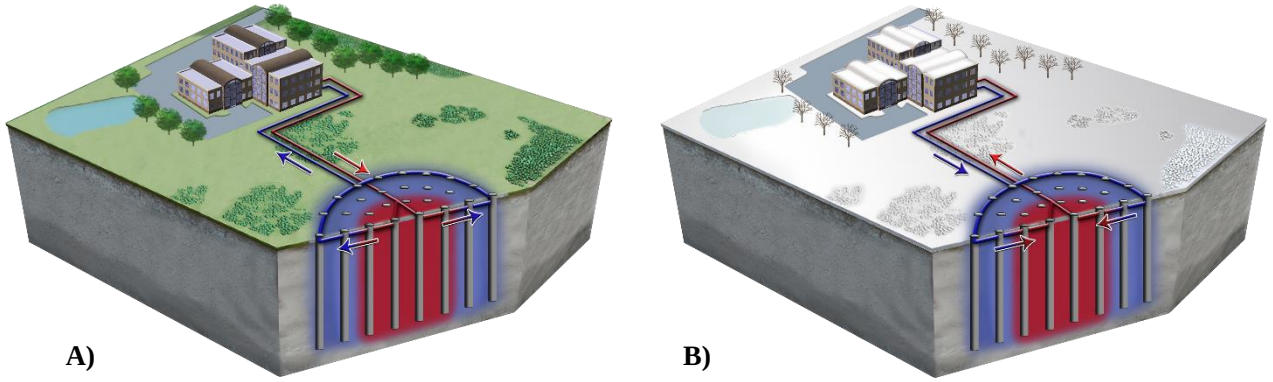

Figure 6 – Diagram of a seasonal underground thermal energy storage system: A) in summer, heat is produced and stored underground; B) in winter, energy is retrieved to heat buildings. The system is a BTES with ground heat exchangers placed in a circular layout (from www.underground-energy.com)

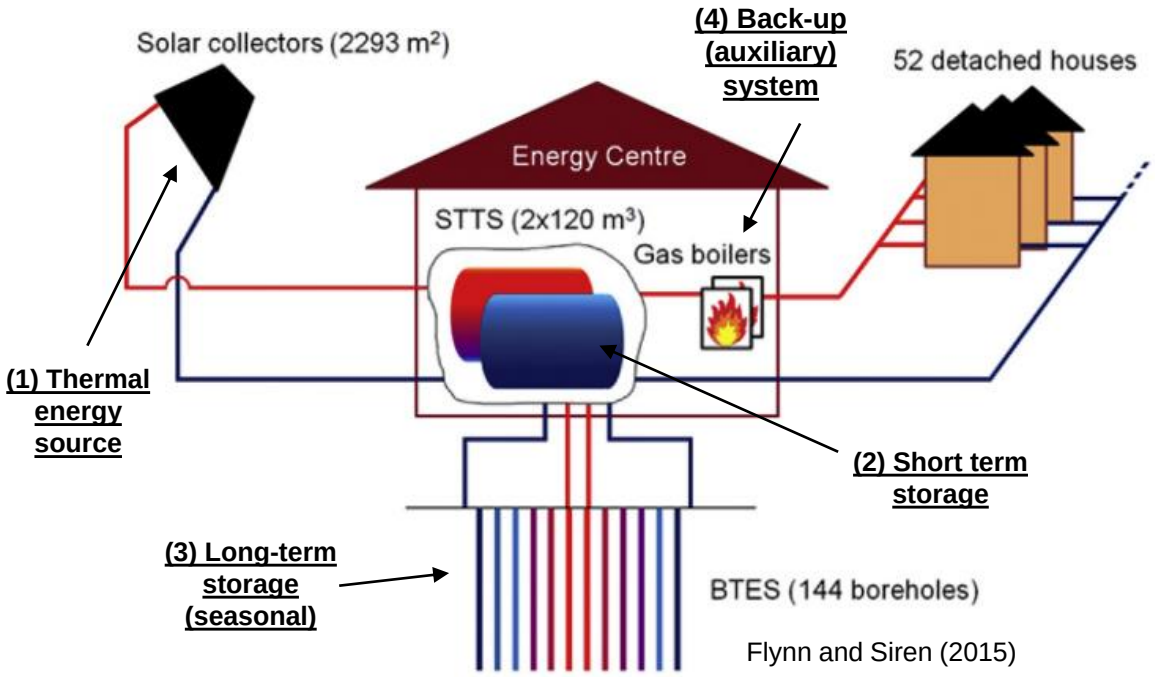

Figure 7 – Diagram of the BTES working at the Drake Landing Solar Community, Okotoks, Alberta (www.dlsc.ca). The 4 basic elements of a TES system are shown.

UNDERGROUND THERMAL ENERGY STORAGE (UTES)

Seasonal underground thermal energy storage (UTES) systems have been conceived in the 1980s to mitigate the intermittency of renewable sources such as solar and wind. These time-dependent supplies do not match with the human needs and the misalignment between the source and the demand is one of the long-standing barriers to renewable sources (such as solar and wind). The peak demand occurs in the late evening and in winter, when the solar radiation is no longer available, while the peak supply takes place in the middle of the day and in summer, when generally both electricity and thermal energy demands are at the minimum. Several plants have been built since the 1980s, with the most active countries being France, Sweden and Switzerland. In the last few decades, Germany has designed and tested a number of central solar heating plants with different types of seasonal storage. Other countries such as China, Canada, Denmark and Italy later contributed to the development of this promising technology. UTES are therefore a mature technology that can help exploit solar energy throughout the whole heating season, thus bridging the gap between the warm and cold seasons (Figure 6A).

Among the several different types of UTES, borehole thermal energy storage (BTES) involves a number of GHE that is conventionally placed in a circular layout in order to create a warm core in the centre (Figure 6B). Differently from the GSHP, the boreholes are shallower (30 - 50 m), such that the entire storage volume is more compact and heat losses toward the surroundings are kept to a minimum. Generally, a thermal recovery of 40 – 60 % can be achieved. This means that if we produce and store 100 GJ in summer, we can most likely retrieve 50 GJ in winter. Subsurface temperature can raise by 20 - 30 °C during the « charge » (warm season) and return back to about its undisturbed value during the «discharge» (cold season). In W-K for instance, the subsurface volume could reach 25 °C at the end of the summer, and return to 3 - 5 °C by the end of the winter.

A typical BTES system, as the one working in Okotoks (Alberta, Figure 7) is made of 4 key elements: (1) a thermal energy source, such as solar collectors (but it can even be some waste heat from a power plant); (2) a short-term storage, normally water tanks; (3) a long-term storage with a series of boreholes; (4) a back-up system to cover peak hours. UTES systems would likely be working even in subarctic conditions characteristic of Whapmagoostui-Kuujjuarapik. Giordano and Raymond (2019) indeed demonstrated that such technology could cover 50 % of the winter energy consumption of the pumping station of the drinking water network in Kuujjuaq.

GEOLOGICAL CONTEXT

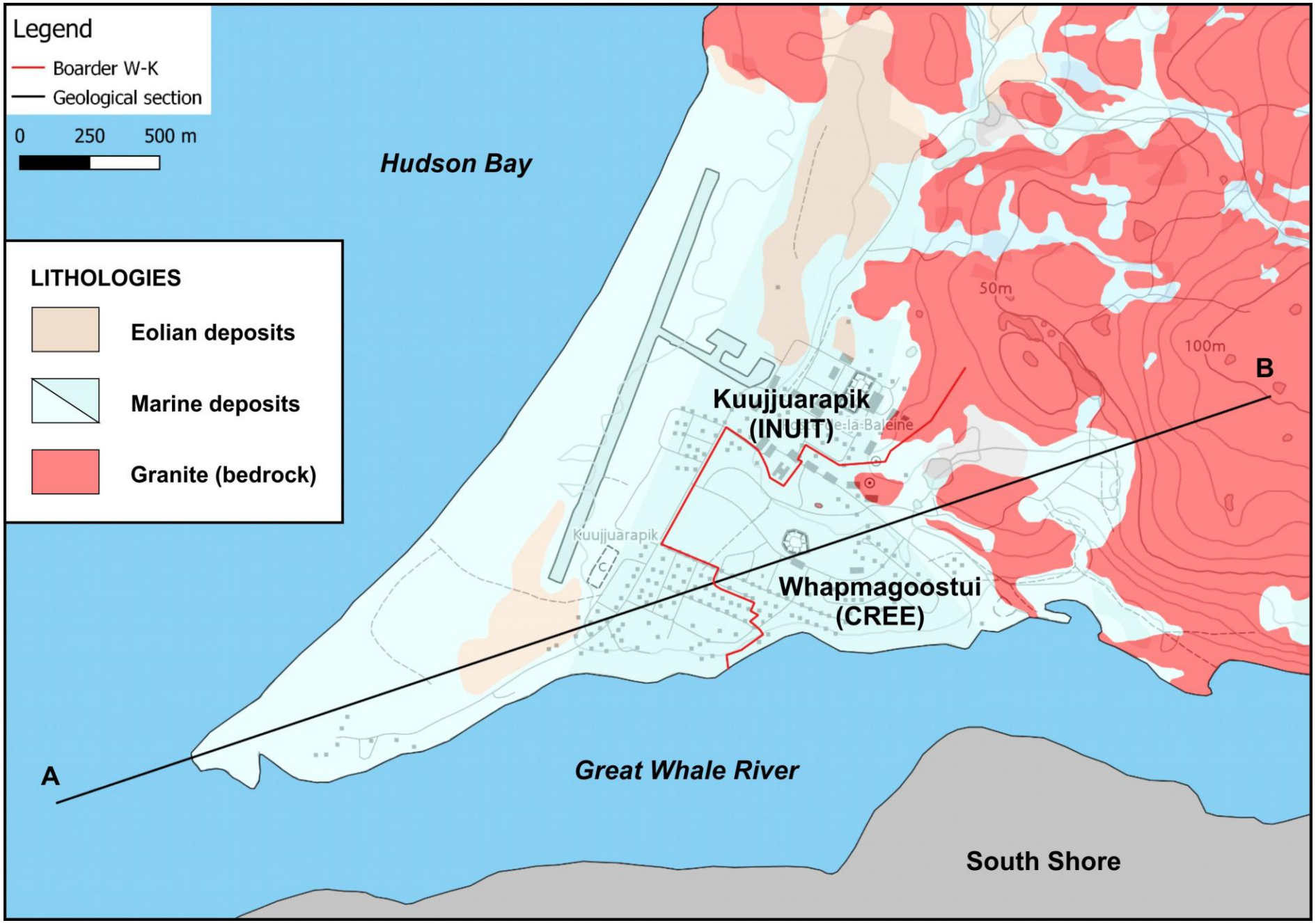

Figure 8 – Geographical and geological setting of W-K (scale 1:16 000). The Inuit population lives in the western and north part of the village, while the Cree population occupies the south-eastern part. The granitic bedrock is highlighted in red. The unconsolidated deposits of the river delta that mainly host the village can be differentiated into marine and eolian deposits (Fortier et al. 2011). The AB line shows the location of the interpreted geological cross-section (Figure 9).

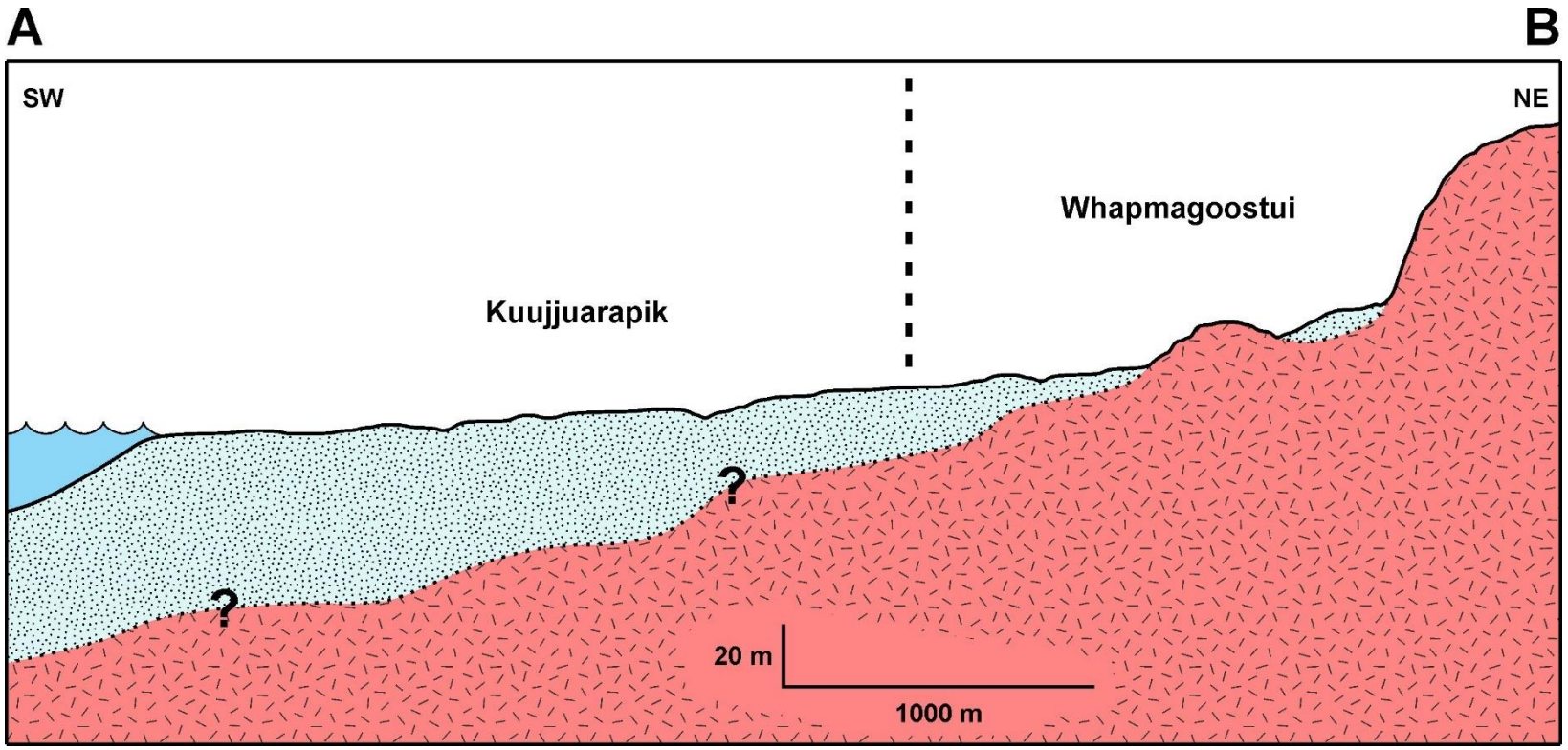

Figure 9 – Geological cross-section of Whapmagoostui-Kuujjuarapik. The location of the AB line is shown in Figure 8.

GEOLOGICAL CONTEXT

From the geological point of view, the northern village of Whapmagoostui-Kuujjuarapik is built on a river delta made of marine deposits that overly the granitic bedrock (Figure 8). The granite formation (Archean age > 2.5 Gy) belongs to the Superior Province of the Canadian Shield and outcrops in the northeastern part of the village. During the last glaciation (> 10 000 y), the glacier had eroded this bedrock and gave it its actual shape, with smoothed hills and small mountains. The bedrock is fairly massive, but fracture sets at the medium scale allows the presence of groundwater that is exploited as the principal drinking source. A number of wells have indeed been drilled in the northeastern hilly part of the village for groundwater research and exploitation.

After the retreat of glaciers, the sea level rose and, with the contribution of the Great Whale River, deposited loamy and sandy sediments that constitute the geological formation on which the village stands (Figure 9). From the bottom, the stratigraphy is made of thin glacial till deposits (1 - 2 m), loamy marine deposits (5 - 15 m) and marine-delta sandy sediments (20 - 30 m). On the surface, those sediments have been reworked by the wind by forming sand dunes typical in the southwestern zones of the village. The total thickness of the unconsolidated deposits on top of the bedrock ranges from a few metres (5 - 10 m) close to the hills, to more than 50 m at the most southwestern parts of the delta.

G.POT PRINCIPLES

GSHPs (ground-source heat pumps) exchange heat with the ground to provide sustainable heating or cooling. Their technological feasibility and economic viability depend on the site-specific thermal properties of the ground and the load of the building to be heated. These parameters influence the shallow geothermal potential, which is defined as the thermal power that can be efficiently exchanged by a BHE (Borehole Heat Exchanger) of a certain depth. We present a general method (G.POT) for the determination of shallow geothermal potential. This method was derived using a comprehensive set of analytical heat transfer simulations, performed by varying (1) the thermal properties of the ground, which comprise its thermal conductivity and capacity, (2) the thermal properties of the borehole, and (3) the operational and design parameters of the heat pump system, namely, the BHE length, the threshold temperature of the heat carrier fluid, the duration of the heating/cooling season and the simulated lifetime. Therefore, the G.POT method is a simple and flexible tool that can be implemented in a wide range of scenarios for the mapping of the shallow geothermal potential (Casasso and Sethi, 2016).

$$P_{\mathrm{BHE}} = \frac{0.0701 \cdot (T_0 - T_{\mathrm{lim}}) \cdot \lambda \cdot L \cdot t'_{\mathrm{c}}}{G_{max}(u'_{\mathrm{s}}, u'_{\mathrm{c}}, t'_{\mathrm{c}}) + (4\pi\lambda \cdot R_{\mathrm{b}})}$$

$$G_{max}(u'_s, u'_c, t'_c) = [-0.619 \cdot t'_{\mathrm{c}} \cdot ln(u'_{\mathrm{s}})] + [(0.532 \cdot t'_{\mathrm{c}} - 0.962) \cdot ln(u'_{\mathrm{c}})] - [0.455 \cdot t'_{\mathrm{c}}] - 1.619$$

$$t'_{\mathrm{c}} = \frac{t_{\mathrm{c}}}{t_{\mathrm{y}}} \qquad u'_{\mathrm{c}} = \frac{\rho c \cdot r_{\mathrm{b}}^2}{4\lambda t_{\mathrm{c}}} \qquad u'_{\mathrm{s}} = \frac{\rho c \cdot r_{\mathrm{b}}^2}{4\lambda t_{\mathrm{s}}}$$

$$R_{\mathrm{b}} = \frac{1}{2\pi\lambda_{\mathrm{bf}}} \cdot ln\left(\frac{r_{\mathrm{b}}}{r_{\mathrm{p}}}\right)$$

P_{BHE}	Closed-loop potential energy	MWh y^{-1}
T_{o}	Initial ground temperature	°C
T_{lim}	Minimum fluid temperature	°C
λ	Ground thermal conductivity	W m^{-1} K^{-1}
ρc	Ground heat capacity	J m^{-3} K^{-1}
L	Borehole length	m
r_{b}	Borehole radius	m
R_{b}	Borehole thermal resistance	m K W^{-1}
t_{c}	Length of heating season	d
t_{y}	Year	d
t_{s}	Simulation time (lifetime)	y
λ_{bf}	Grout thermal conductivity	W m^{-1} K^{-1}
n	Number of pipes	–
r_{p}	Pipe radius	m

Energy stored

$$Q_{STO} = f(\lambda, \rho c) \begin{cases} \lambda = f(bedrock\ and\ groundwater\ depth) \\ \rho c = f(bedrock\ and\ groundwater\ depth) \end{cases}$$

Heat losses

$$Q_{LOST} = f(\lambda, \rho c, groundwater\ depth\ and\ Darcy\ velocity)$$

Available energy

$$Q_{REC} = Q_{STO} - Q_{LOST}$$

Thermal recovery

$$\eta = Q_{REC}/Q_{STO}$$

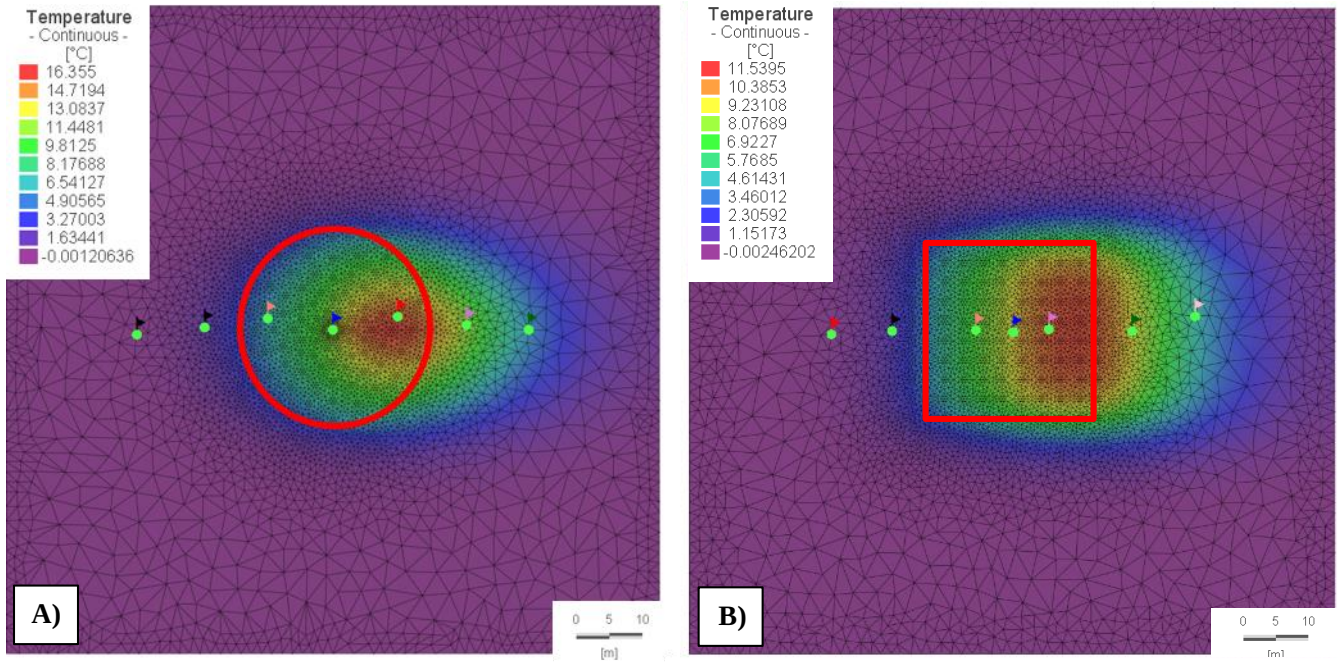

Figure 10 – Numerical simulations of the thermal energy storage systems in the underground allow quantifying for the heat lost owing to the groundwater flow. The losses can be reduced by optimizing the volume of storage, which can be either of cylindrical (A) or square shape (B) (Giordano and Raymond, 2019).

STOREmap PRINCIPLES

The STOREmap method takes into account the subsurface thermal and physical properties to evaluate the amount of energy that can be stored into the underground (Q_{STO}). This amount is strongly related to the depth of the bedrock and the groundwater table. Indeed, these last parameters have a significant influence on both the thermal conductivity and the heat capacity, and thus on the thermal diffusivity of the storage volume. Thermal conductivity (λ) is a property that quantifies the amount of heat that is transferred by a medium; heat capacity (ρc) defines the amount of thermal energy that can be stored in a medium; thermal diffusivity is the ratio of the two (conductivity / heat capacity) and describes the velocity of the heat diffusion. The unconsolidated sediments have lower λ than the bedrock (1.5 – 2 times), but higher ρc (1.5 – 1.6 times). Moreover, the presence of water in the sediments increases both conductivity and heat capacity. Therefore, it is clear that the delta deposits and the bedrock are two thermal units with very different behaviours, in particular if the first are saturated (below the water table).

Those parameters also impact the amount of energy that would be lost during the charge of the system (Q_{LOST}). The most important element is actually the velocity of the groundwater (Darcy's velocity), that is a function of the medium's hydraulic conductivity and the local hydraulic gradient. Indeed, if the groundwater is moving due to the hydraulic head distribution, the system is not only controlled by heat conduction. The heat transport caused by the advection must thus be taken into account, because this is significantly more important than the heat transfer occurring by conduction only. Unfortunately, the Darcy velocity is one of the most difficult parameters to evaluate in the field, because at least three wells are necessary to define the main direction of the flow and then quantify its magnitude. According to Giordano and Raymond (2019), with a Darcy velocity of 10^{-6} m s^{-1}, the heat transport by advection contributes with an additional 10 % of the total Q_{LOST}. This Darcy velocity is the result of a hydraulic gradient of 1.5 % and hydrogeological conditions very similar to the W-K setting. Once Q_{STO} and Q_{LOST} are evaluated, the thermal recovery (η) can be estimated and different layouts of the underground storage volume can be tested to optimize the system and increase the overall effectiveness (Figure 10; Giordano and Raymond, 2019).

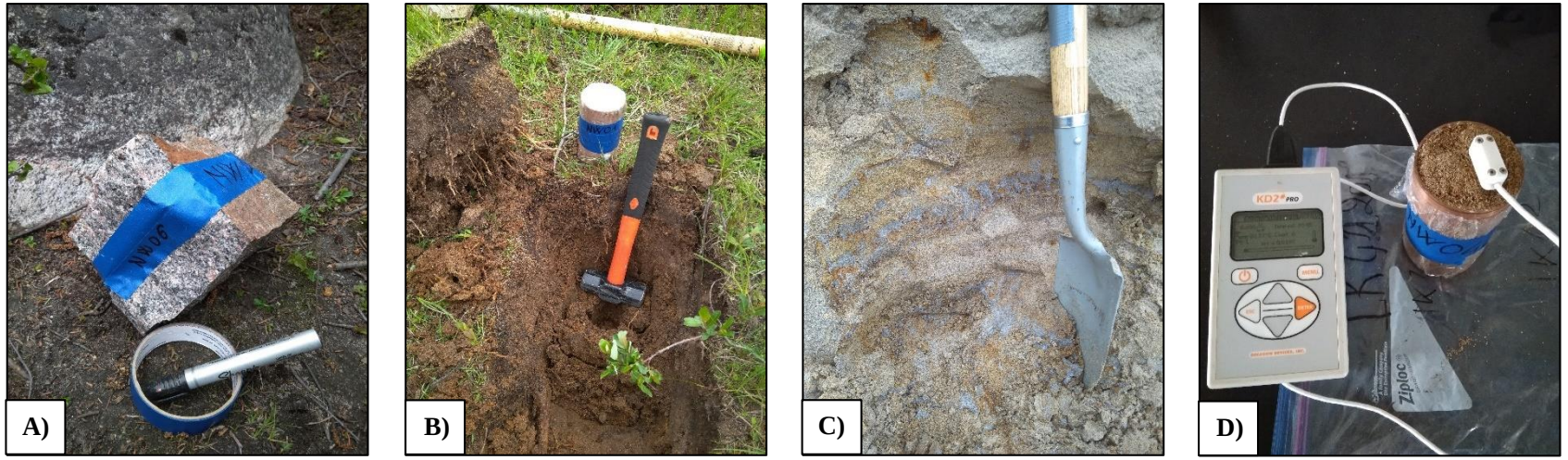

Figure 11 – Sampling of rock formations (A) and unconsolidated sediments (B, sandy delta deposits; C, loamy-sandy marine deposits). D) Analysis of thermal conductivity and volumetric heat capacity of unconsolidated sediments with the needle probe KD2 Pro.

http://log.ete.inrs.ca/

log laboratoire ouvert de géothermie

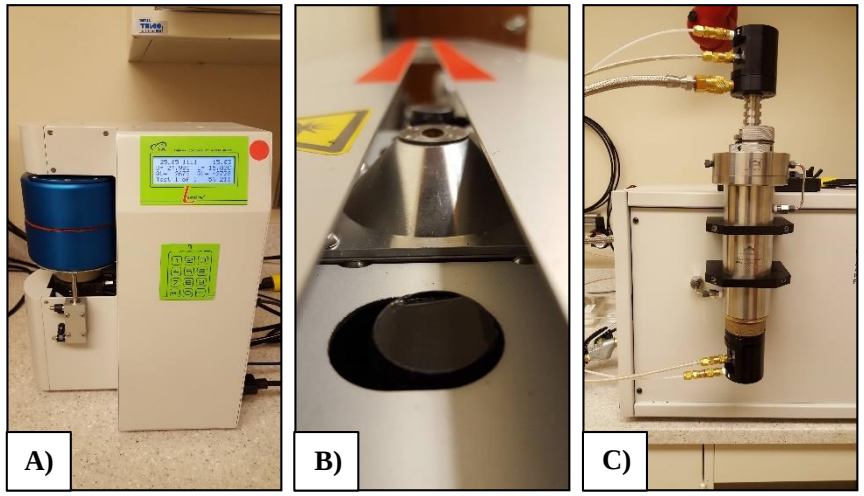

Figure 12 – Instruments for measuring thermal and physical properties of rock formations available at INRS Open Geothermal Laboratory (LOG): guarded heat flow meter (A), thermal conductivity scanner (B) and the gas porosimeter/permeameter (C).

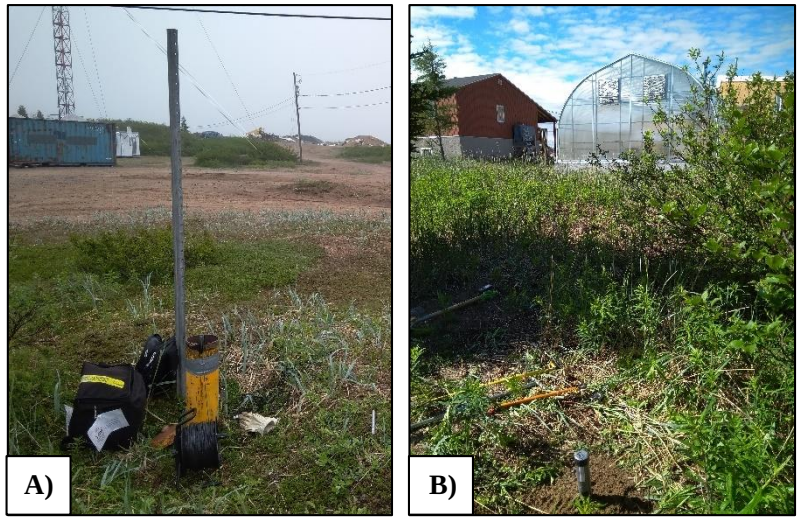

Figure 13 – Measurement and monitoring of the underground temperature. A) A temperature log was carried out in well TF05-07 (geographic coordinates 55.27 N 77.75 W, depth 120 m), one of the wells drilled for groundwater research. B) TW1 is a piezometer installed at the CEN Station in 2018 for shallow ground temperature annual monitoring (measuring depths 50 and 70 cm).

FIELD AND LAB ACTIVITIES

Field activities have been carried out in the village and its surroundings in 2018 and 2019 in order to evaluate the potential of installing geothermal technologies in Whapmagoostui-Kuujjuarapik. In particular, sampling of the rock formations (Figure 11A, 2 samples) and the unconsolidated sediments (Figure 11B-C, 9 samples) is crucial to measure the in situ thermal conductivity, volumetric heat capacity, porosity and permeability. As aforementioned, the same rock formation outcrops in the area and we believe that it is homogeneous and similar when exposed at the surface (East) or covered by the delta deposits (West). The two samples collected are therefore assumed to be representative of the entire bedrock with a high degree of confidence. On the other hand, the unconsolidated sediments are more heterogeneous, and more samples were needed for a detailed characterization of the shallowest subsurface.

Laboratory measurements were carried out with different instruments: a needle probe for thermal analysis of the sediments (Figure 11D); a guarded heat flow meter to evaluate the influence of temperature on thermal properties from permafrost to reservoir conditions (Figure 12A); an infrared scanner to evaluate the heterogeneity of the thermal properties (Figure 12B); a gas porosimeter/permeameter for the physical and hydraulic properties (Figure 12C).

The temperature of the subsurface and the groundwater depth are other critical parameters for the estimation of the amount of energy that can be extracted from and stored into the underground. Temperature logs were measured in 5 groundwater wells (e.g., Figure 13A) and some sensors were placed in the shallow subsurface (Figure 13B) to monitor the temperature year-long evolution of the ground-atmosphere interface that is highly influenced by the snow cover in winter.

FIELD ACTIVITIES

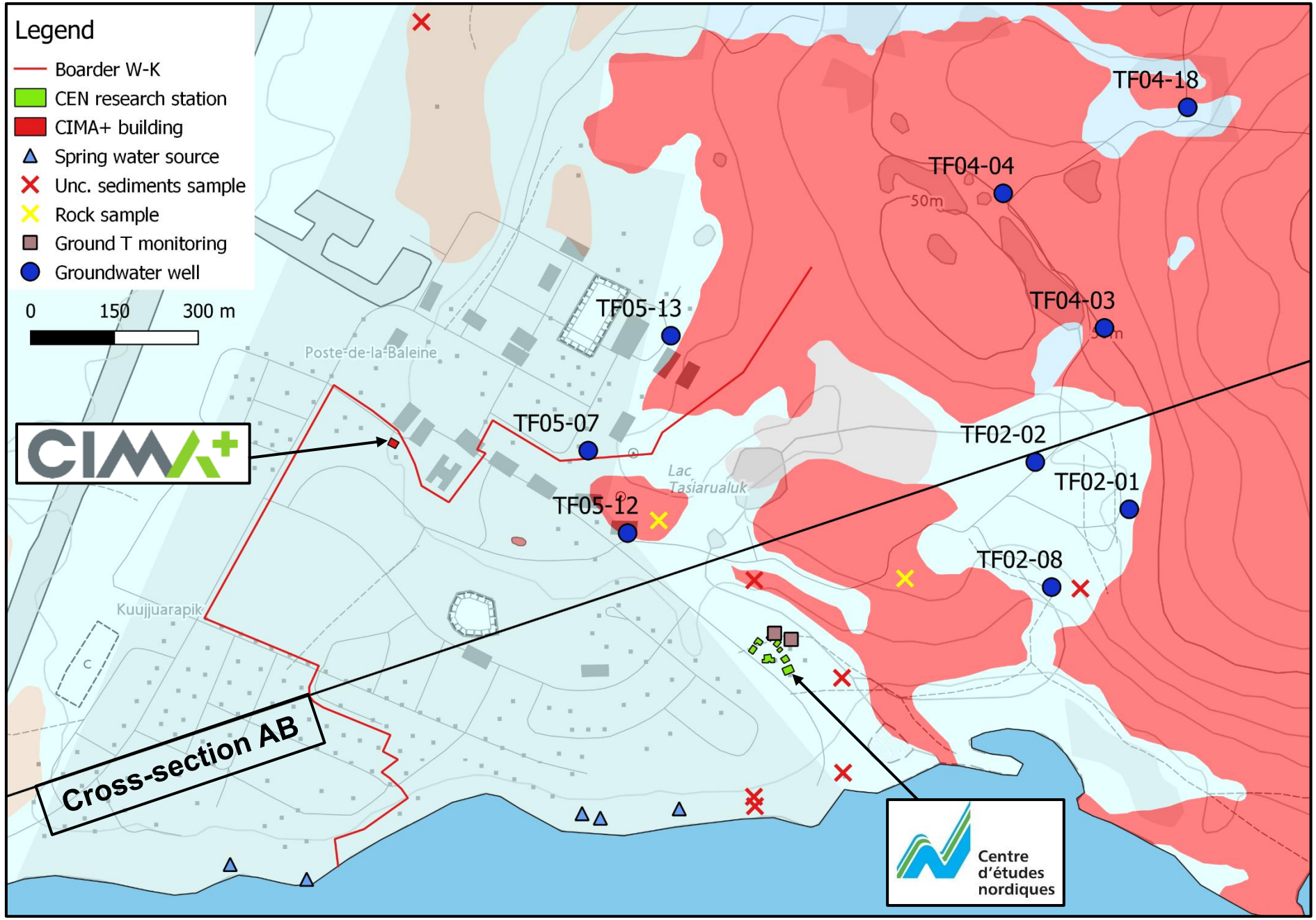

Figure 14 – Location of the groundwater wells, rock and unconsolidated sediment samples, monitoring piezometers and springs (Scale 1:8000). The buildings of CIMA+ and the CEN research station are also highlighted.

Table 1 – Data of groundwater wells shown in Figure 14 (Tiré d'AquaTer-eau, 2014).

Well	Elevation (m)	Depth (m)		Thickness (m)		Water table (m)	
		Relative	Elevation	Unc. sed.	Granite	Depth	Elev.
TF02-01	41	107	-65	3	103	17	24
TF02-02	38	100	-62	15	85	21	18
TF02-08	25	91	-66	12	80	6	20
TF04-03	52	123	-70	0	123	30	23
TF04-04	53	107	-54	0	107	31	22
TF04-18	68	107	-39	0	107	39	30
TF05-07	26	123	-97	9	113	19	7
TF05-12	23	43	-20	6	37	14	8
TF05-13	28	123	-95	2	121	14	13

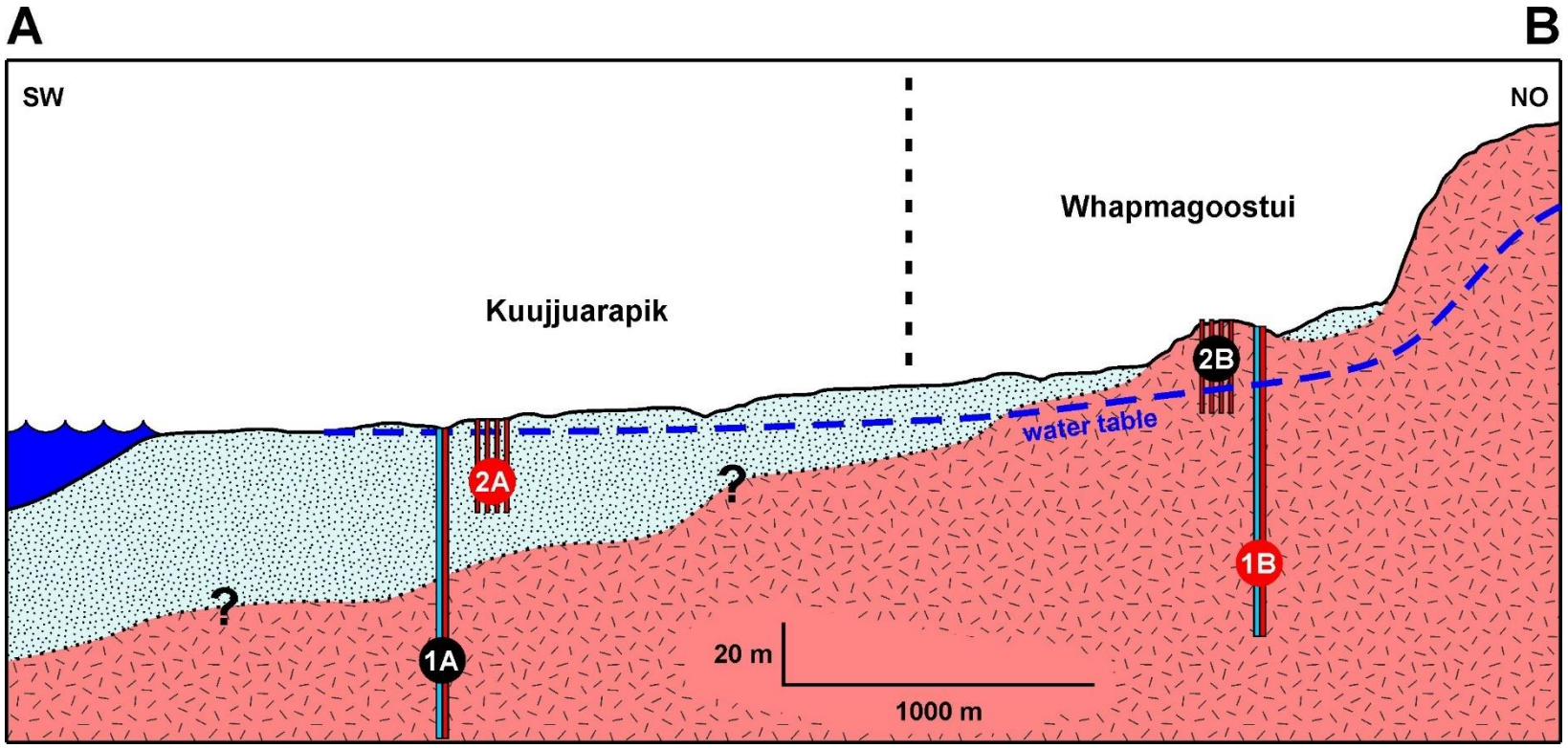

Figure 15 – Geological cross-section of Whapmagoostui-Kuujjuarapik showing the configurations of both GSHP (1) and UTES (2) to obtain the optimistic (in red) and pessimistic (in black) scenarios for a shallow geothermal energy use.

GSHP AND UTES SCENARIOS

Due to a lack of information on the unconsolidated sediments thickness and the depth of the water table in the southwestern part of Whapmagoostui-Kuujjuarapik (Figure 14; Table 1), two different geological configurations were identified for both GSHP and UTES. In this way, optimistic and pessimistic scenarios for shallow geothermal energy potential were defined (Figure 15).

For the GSHP, the optimistic scenario (1B) is when the borehole is completely installed in the bedrock, because the thermal conductivity is higher in this geological medium compared to the unconsolidated sediments. On the other hand, the pessimistic scenario is where the borehole is installed in the thickest part of the unconsolidated sediments. The geological configuration is 50 m of bedrock and 50 m of unconsolidated sediments, as their greatest thickness is estimated to around 50 m, and the GSHP borehole would have 100 m length.

For the UTES, the optimistic scenario (2A) is where the boreholes are installed in the thickest part of the unconsolidated sediments, because the heat capacity is higher in this geological unit compared to the bedrock. As UTES boreholes would have 30 m length, then the geological configuration is 100 % of unconsolidated sediments. On the other hand, the pessimistic scenario (1B) is when boreholes are installed entirely in the bedrock.

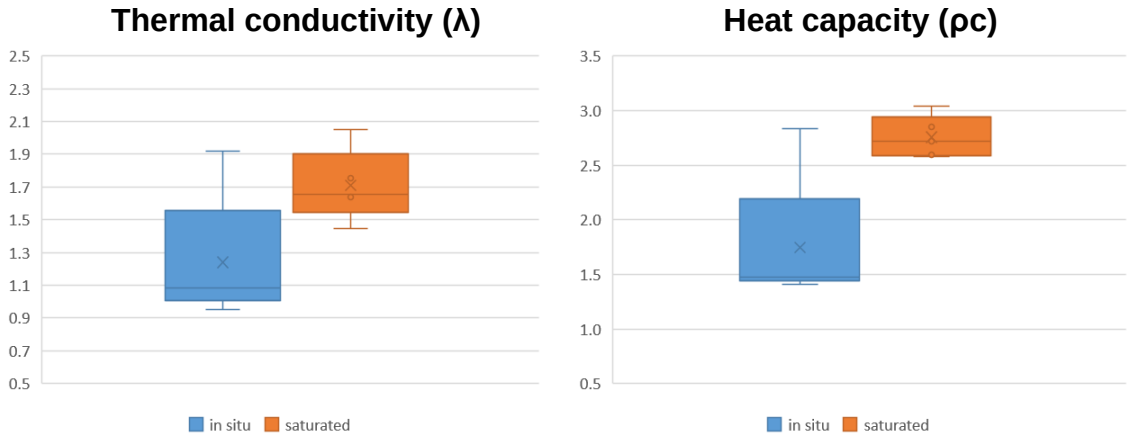

Figure 16 – Thermal property assessment of unconsolidated sediments. In situ results refer to the samples analyzed as they were collected in the field. The samples were then completely saturated with tap water to represent the conditions below the water table.

	Thermal conductivity ($W\ m^{-1}\ K^{-1}$)	St. dev.	Thermal diffusivity ($10E\text{-}6\ m^2\ s^{-1}$)	St. dev.	Heat capacity ($MJ\ m^{-3}\ K^{-1}$)
NW05	2.958	0.034	1.286	0.038	2.300
NW06	2.920	0.087	1.300	0.098	2.246

Figure 17 – Thermal property assessment of the two granite samples.

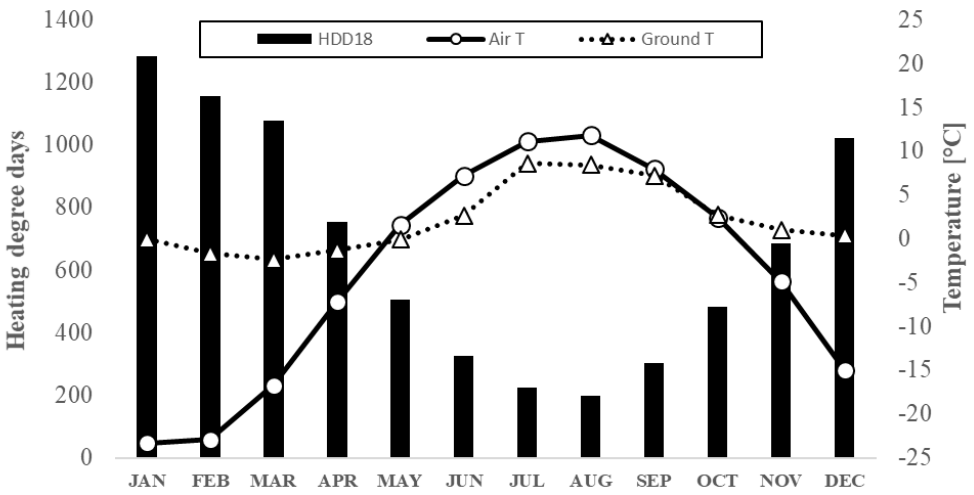

Figure 19 – Temperature measured at the interface ground/atmosphere (50 cm depth) during the 2018-2019 season. This trend is compared with the atmospheric temperature and the heating degree days in W-K.

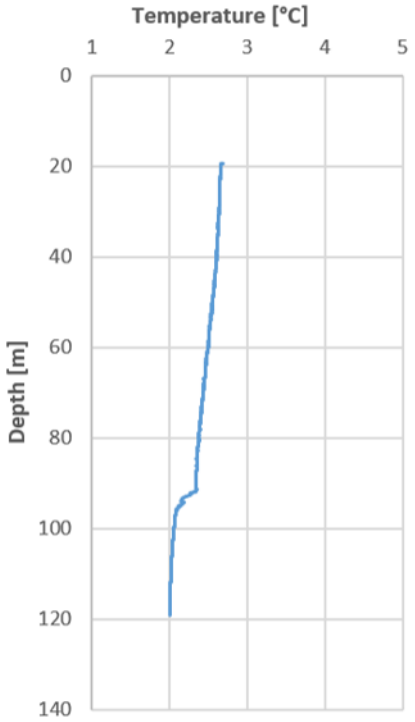

Figure 18 – Temperature log measured in TF05-07.

THERMAL PROPERTIES

The results of the thermal property assessment show that thermal conductivity of the unconsolidated sediments ranges from 1.1 to 1.5 W m^{-1} K^{-1} and from 1.5 to 1.9 for the in situ and saturated conditions, respectively (Figure 16). As expected, the heat capacity is similarly lower in situ (1.5 – 2.0 MJ m^{-3} K^{-1}) and fairly higher when the sample is completely saturated with water (2.6 – 2.9 MJ m^{-3} K^{-1}). The high internal variability is mainly related to the different water contents, but also to the characteristic porosity values related to the grain-size distributions of the sandy and loamy sediments. On the other hand, the granite of the bedrock show fairly homogeneous values as expected, with 2.9 W m^{-1} K^{-1} and 2.3 MJ m^{-3} K^{-1} (Figure 17). Its primary porosity is less than 1 %, showing the massive nature of the matrix. The permeability that allows the exploitation of the bedrock for drinking purposes is indeed due to the secondary porosity consisting of fractures and joints related to ancient geodynamic processes. There can also be near-surface fractures due to isostatic rebound.

The thermal diffusivity is around 1.3 x 10^{-6} m^2 s^{-1} in the granite and 0.6 - 0.7 x 10^{-6} m^2 s^{-1} in the sediments, whether saturated or not, respectively. This gives a clear idea that the bedrock (high diffusivity) is the target medium for ground-source heat pumps, while the sediments (low diffusivity), in particular if saturated, are the best option for thermal energy storage systems. Indeed, the first technology requires a more efficient (fast) heat extraction, while the latter necessitates a medium more prone to accumulate the heat and limit the losses.

The undisturbed underground temperature shows no evidence of permafrost, being near 2 – 2.5 °C in the first 120 m b.g.l. (Figure 18). It is rather evident that the snow cover plays a key role of insulation, limiting the minimum winter temperature to -2.3 °C (Figure 19).

G.POT RESULTS

For the GHSP scenarios, the G.POT method was used with the thermal properties values listed in Table 2. The results show that one 100-m-deep borehole heat exchanger (P_{BHE}) could provide between 10.7 and 13.2 MWh per year, for pessimistic (1A) and optimistic (1B) scenarios, respectively.

If that energy was extracted by a compression heat pump with a COP of 3 (Gunawan et al, 2020), we would need from 4 to 5 boreholes to cover the heating need of the reference building (70 MWh y^{-1}; Figures 2 and 3). The total energy that we need to extract from the underground (P_{ground}) is 46.7 MWh y^{-1} and is calculated with:

$$P_{ground} = P_{building}\left(\frac{COP - 1}{COP}\right)$$

In brief, the pessimistic scenario (1B) would be 25% less efficient than the optimistic scenario (1A, Table 3).

Table 2 – Thermal conductivity and heat capacity values used for the GSHP scenarios according to the geological configurations in Figure 15.

Ground source heat pumps (GSHP)			
Scenario 1A	**%**	**Thermal cond.**	**Heat cap.**
Bedrock	50	3,00	2,30
Unconsolidated sediments	50	1,70	2,70
		2,35	**2,50**
Scenario 1B			
Bedrock	100	**3,00**	**2,30**

Table 3 – Results of the GSHP scenarios

		1B Optimistic		1A Pessimistic	
Initial ground temperature	T_o	2		2	°C
Minimum fluid temperature	T_{lim}	-5	°C	-5	°C
Ground thermal conductivity	λ	3,00	W m^{-1} K^{-1}	2,35	W m^{-1} K^{-1}
Ground heat capacity	ρc	2,30	J m^{-3} K^{-1}	2,50	J m^{-3} K^{-1}
Borehole length	L	100	m	100	m
Borehole radius	r_b	0,076	m	0,076	m
Length of heating season	t_c	365	days	365	days
Year	t_y	365	days	365	days
Simulation time (lifetime)	t_s	25	years	25	years
Grout thermal conductivity	λ_{bf}	1,50	W m^{-1} K^{-1}	1,50	W m^{-1} K^{-1}
Number of pipes	n	2	-	2	-
Pipe radius	r_p	0,017	m	0,017	m
	t'_c	1,00		1,00	
	u'_c	0,00		0,00	
	u'_s	0,00		0,0001	
	G_{max}	9,59		9,25	
	$r_{p,eq}$	0,02		0,02	
Borehole thermal resistance	R_b	0,12	m K W^{-1}	0,12	m K W^{-1}
Closed-loop potential energy	P_{BHE}	13,23	MWh y^{-1}	10,69	MWh y^{-1}
Reference building	$P_{building}$	70	MWh y^{-1}	70	MWh y^{-1}
Coefficient of performace	COP	3,00		3,00	
Total geothermal energy	P_{ground}	46,67	MWh y^{-1}	46,67	MWh y^{-1}
Number of boreholes needed		4		5	

STOREmap RESULTS

We considered a total energy need of 350 MWh for UTES, corresponding to a complex of 5 buildings in a small district heating network. Let's assume a general UTES system with an underground storage volume of 24 000 m^3, which means a cylinder with both diameter and depth of 30 m, as proposed by Giordano and Raymond (2019).

Table 4 – Results of the UTES scenarios

Underground thermal energy storage (UTES)		Thermal conductivity	Heat capacity	Thermal diffusivity	Storage volume	Average temperature	η	Q_{STO}	Q_{REC}	Q_{LOST}	Coverage
Scenario 2A	%	W m^{-1} K^{-1}	MJ m^{-3} K^{-1}	m^2 s^{-1}	m^3	°C	%	GJ	GJ	GJ	%
Unconsolidated sediments	100	1.70	2.70	0.63	24000	15.2	55%	935	510	425	54%
Scenario 2B											
Bedrock	100	3.00	2.30	1.30	24000	17.5	50%	917	454	463	48%

Let's also consider having 1000 GJ (ca. 278 MWh) of thermal energy that we want to store for later use. This energy can be produced by whatever means, such as renewable sources (solar, wind, hydro) or waste heat (power plant), and is not going to be discussed further since it is beyond the scope of the present report. This amount of heat will increase the temperature of the storage on average by 15 - 17 °C during the charging phase (Table 4). Through analytical calculations calibrated with numerical models, the thermal recovery of scenario 2A is estimated to be about 57 %, while in the bedrock would be approximately 50 % (2B). This is due to the different thermal diffusivity, higher in the bedrock than in the saturated delta-marine sediments. As aforementioned, when the heat transfer mechanism is driven only by conduction, the heat losses depend only on this factor. When the groundwater flow cannot be neglected, such as in the present case, the contribution of the groundwater advection must be considered as a means of heat loss. By taking into account the maximum possible hydraulic gradient expected at the site (0.8 %, Figure 20), the thermal recovery of scenario 2A decreases approximately by 2 %, and is estimated to drop to 55 % (Giordano and Raymond, 2019). The energy recovered during the discharge phase is therefore 510 and 454 GJ in scenario 2A and 2B, respectively (Table 3). The reference compression heat pump would have a COP of 4 (Gunawan et al., 2020), bigger than the one considered in the GSHP scenarios since the temperature of the fluid feeding the heat pump can be higher (more than 10 °C). In conclusion, this system is able to cover 54 % (2A) and 48 % (2B) of the energy demand of the building complex. It is important to note that, for simplicity, scenario 2A is considered to be hosted in unconsolidated sediments completely saturated by groundwater. Clearly, this is not always the case, in particular in the Cree territory of Whapmagoostui (see cross section in Figure 15). Since the heat capacity of dry unconsolidated sediments is 1.7 MJ m^{-3} K^{-1}, the estimated thermal recovery would only be 30 %, making this scenario far from being technically and economically reasonable. Therefore, we can conclude that when the depth of the water table is more than 10-15 m, the UTES system would have to be deeper than the 30 m considered in this calculation. As a design rule of thumb, we can say that at least 2/3 of the UTES depth should be below the water table.

The spreadsheet "STOREmap.xlsx" has been built and used for these calculations (Annex 1).

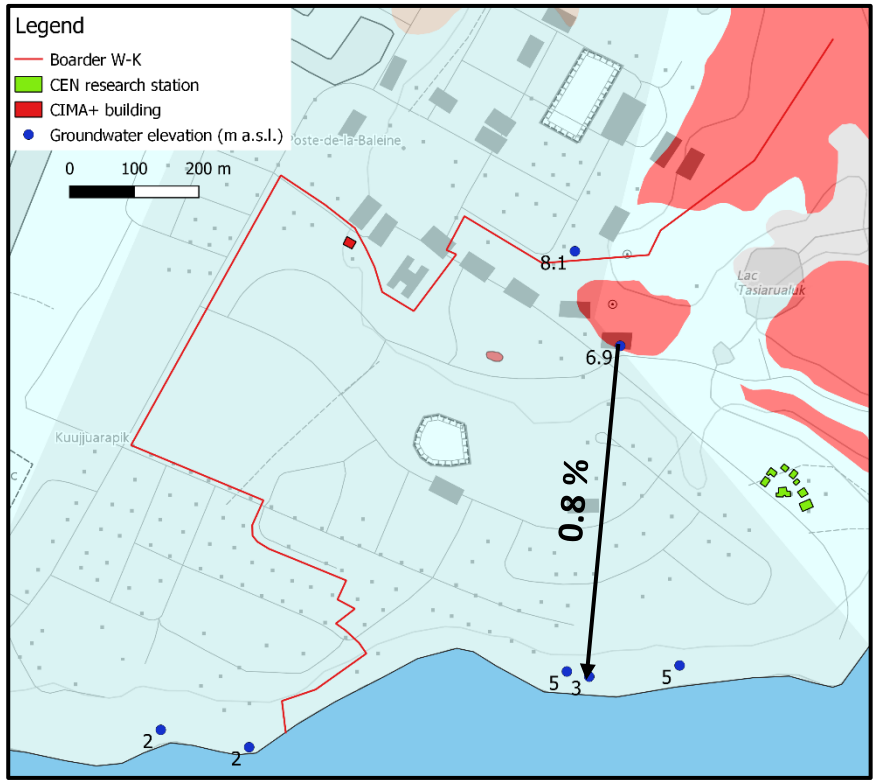

Figure 20 – Location of the available groundwater elevation data and indication of the maximum hydraulic gradient expected at the site (Scale 1:6000).

CONCLUSIONS

- The northern village of Whapmagoostui-Kuujjuarapik was studied for its shallow geothermal energy potential for heating purposes.
- The main uncertainties are the thickness of the unconsolidated sediments over the bedrock and the depth of the water table in the southwestern part of the village.
- Due to these uncertainties, it was not possible to provide a detailed mapping of the shallow geothermal potential of the village.
- Therefore, from a geological point of view, two main configurations (scenarios) were distinguished: the granite bedrock and the unconsolidated sediments, in the northeastern and southwestern parts of the village.
- The field activities carried out in the summers of 2018-2019 allowed us to characterize both geological units from a thermo-hydrogeological point of view.
- The saturated unconsolidated sediments (1.7 W m^{-1} K^{-1}) have a thermal conductivity lower than the bedrock (2.9 W m^{-1} K^{-1}), but higher heat capacity (2.7 vs. 2.3 MJ m^{-3} K^{-1}). Therefore, it is clear that the delta deposits and the bedrock are two thermal units with very different behaviours, in particular if the first are saturated (below the water table).
- Basically, we can say that the bedrock (high diffusivity) is the target medium for ground-source heat pumps, while the sediments (low diffusivity), in particular if saturated, are the best option for thermal energy storage systems.
- The undisturbed ground temperature is evaluated to be near 2 - 2.5 °C in the shallowest 100 metres.
- For the ground-source heat pump (GSHP), the best configuration is when BHEs are completely in the bedrock. One 100-m-deep borehole can guarantee 13.2 MWh y^{-1}, which is 25 % more than the worst scenario, where the unconsolidated sediments are expected to be the thickest (around 50 m).
- According to these scenarios, 4 and 5 boreholes are anticipated to be necessary to cover the total heating need of the reference building (70 MWh y^{-1}) with a compression heat pump (COP of 3).
- For the underground thermal energy storage (UTES), the best configuration is completely in the saturated unconsolidated sediments, that guarantee a thermal recovery of 55 %. The worst-case scenario (in the bedrock) can, however, allow recovering 50 % of the energy stored during the charge phase.
- The total heating needs of a small district heating system (5 reference buildings, 350 MWh y^{-1}) can be covered at 54 % and 48 % by a UTES system installed in the saturated unconsolidated sediments and in the bedrock, respectively.
- **Shallow geothermal energy technologies (GSHP and UTES) are technically feasible in the subarctic setting of Whapmagoostui-Kuujjuarapik. A 100-m-deep BHE drilled in any part of the village can provide on average 12 ± 1.3 MWh y^{-1} for a ground-source heat pump. An underground thermal energy storage system can assure that at least 50 ± 5 % of the energy is recovered during the winter season.**

FUTURE WORKS

- At least one borehole will have to be drilled in the southwestern part of the village in order to evaluate the thickness of the unconsolidated sediments and the water table depth, and then reduce the main uncertainties highlighted in this study.
- The thermo-physical characterization carried out in this work only relies on surface samples. Therefore, this borehole is also critical to estimate the thermal properties all along its length, in order to better evaluate the amount of energy that can be extracted and stored.
- A life-cycle cost analysis can be carried out as a further step for both GSHP and UTES in order to define the economical feasibility compared to the current diesel-dependent situation of northern villages in Québec.
- Coupling geothermal energy with other renewable sources, such as biomass, solar and wind, is an interesting option to study in the future.

REFERENCES

AquaTer-Eau, 2014. Amélioration du système d'approvisionnement d'eau potable - Première Nation Crie de Whapmagoostui et Communauté Inuit de Kuujjuarapik - Recherche en eau souterraine et construction du puits P-2. Rapport hydrogéologique ATE-12162-01, 216 p.

Belzile, P., Comeau, F.-A., Raymond, J., Lamarche, L., Carreau, M., 2017. Arctic climate horizontal ground-coupled heat pump. Transactions - Geothermal Resources Council 41: 1958-1978.

Casasso, A. and Sethi, R., 2016. G.POT: A quantitative method for the assessment and mapping of the shallow geothermal potential. Energy 106:765-773. http://dx.doi.org/10.1016/j.energy.2016.03.091

Flynn, C., Siren, K., 2015. Influence of location and design on the performance of a solar district heating system equipped with borehole seasonal storage. Renewable Energy, 81: 377–388. https://doi.org/10.1016/j.renene.2015.03.036

Fortier, R., Allard, M., Lemieux, J.-M., Therrien, R., Molson J. and Fortier. D., 2011. Cartographie des dépôts quaternaires des villages nordiques de Whapmagoostui-Kuujjuarapik, Umiujaq, Salluit et Kuujjuaq. Rapport de synthèse de la phase I, Ministère de l'Énergie et des Ressources naturelles, Québec, MB 2011-12, 122 p. http://gq.mines.gouv.qc.ca/documents/EXAMINE/MB201112/

Giordano, N. and Raymond, J., 2019. Alternative and sustainable heat production for drinking water needs in a subarctic climate (Nunavik, Canada): Borehole thermal energy storage to reduce fossil fuel dependency in off-grid communities. Applied Energy 252:113463. https://doi.org/10.1016/j.apenergy.2019.113463

Gunawan, E., Giordano, N., Jensson, P., Newson, J., Raymond, J., 2020. Alternative heating systems for northern remote communities: Techno-economic analysis of ground-coupled heat pumps in Kuujjuaq, Nunavik, Canada. Renewable Energy 147: 1540-1553. https://doi.org/https://doi.org/10.1016/j.renene.2019.09.039.

Moran, M.J., Shapiro, H.N., Boettner, D.D., Bailey, M. B., 2018. Fundamentals of engineering thermodynamics. John Wiley & Sons Ltd., 9th Ed., Chichester, 1004 pp.

Raymond, J., 2018. Colloquium 2016: Assessment of the subsurface thermal conductivity for geothermal applications. Canadian Geotechnical Journal, 55(9): 1209-1229. https://doi.org/10.1139/cgj-2017-0447

Société du Plan Nord [online]. Map 6 : Electricity generation in the area covered by the Plan Nord. http://plannord.gouv.qc.ca/wp-content/uploads/2015/04/Carte-6-ANG.pdf

ACKNOWLEDGMENTS

This project was funded by a Engage grant of the Natural Sciences and Engineering Research Council of Canada (NSERC).

CRSNG
NSERC

Finally, we would like to thank the Cree Nation Government and the Whapmagoostui First Nation for authorizing the transfer of the hydrogeological reports from CIMA+, which made this research work possible.

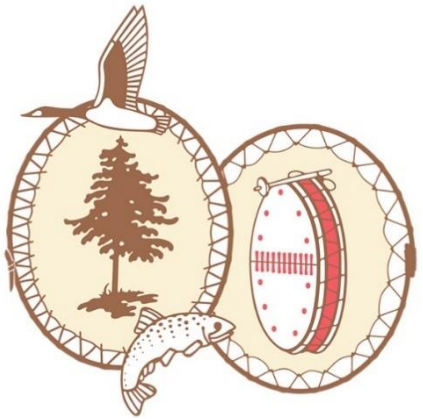

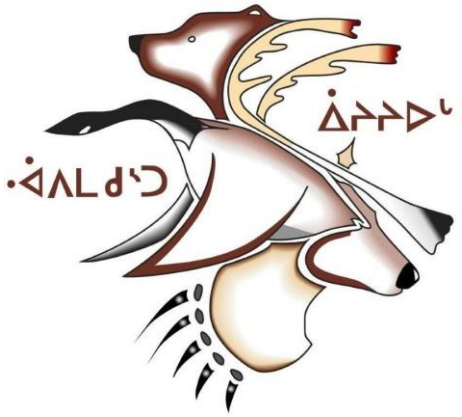

APPENDICE 1 - STOREMAP

Energy setting	
Energy demand [MWh]	350
Energy demand [GJ]	1260
Solar production [GJ/m2]	3,00
Solar collectors efficiency	0,3
Solar area [m2]	1000
N solar panels [-] (2 m2 each)	500
Energy production [GJ]	900,0
ST losses [-]	0,05
Injected in the BTES [GJ]	855,0

	Scenarios		
Geological setting	**2b**	**2a**	**Calibration**
Cv ground [MJ/m3/K]	2,3	2,7	3
λ ground [W/m/K]	3	1,7	1,5
eff. porosity [-]	0,05	0,35	0,35
K [m/s]	1,00E-08	1,30E-05	5,00E-05
Hydraulic gradient [%]	1,5%	0,8%	1,5%
Undisturbed T ground [°C]	2	2	0
Heat transfer thickness [m]	3,40	1,93	1,70
6 months [s]	15552000	15552000	15552000
Part of energy in the warm core [-]	0,4	0,4	0,4
Part of energy in the annulus [-]	0,6	0,6	0,6
			TC/thickness
			1,13

	Scenarios			
	2b	**2a**	**Notes**	**Calibration**
N bhe [-]	100	100		100
Depth [m]	30	30		30
Total L bhe [m]	3000	3000		3000
Spacing [m]	3,0	3,0		3,0
shape [-]	cylinder	cylinder		cylinder
BTES volume [m3]	24000	24000		24000
diameter [m]	31,9	31,9		31,9
radius [m]	16,0	16,0		16,0
Side area [m2]	3007,98	3007,98		3007,98
Top/bottom area [m2]	800,02	800,02		800,02
surface area to volume ratio [m-1]	0,192	0,192		0,192
ideal shape scenario [m-1]	0,193	0,193		0,193
difference %	-0,33%	-0,33%	Be sure that this value be within ± 1%	-0,33%
T BTES average [°C] (homogneou	17,5	15,2		11,9
Stratified case				
Energy warm core [GJ]	342,0	342,0		342,0
Energy annulus [GJ]	513,0	513,0		513,0
Volume of warm core [m3]	2666,72	2666,72		2666,72
Volume of annulus [m3]	21333,75	21333,75		21333,75
T warm core [°C]	57,8	49,5		42,7
T annulus [°C]	12,5	10,9		8,0
Conduction				
Side area warm core [m2]	1002,66	1002,66		1002,66
Rate core-to-annulus [kW]	40,08	34,14		30,73
Energy core-to-annulus [GJ]	623,34	531,00		477,90
Rate annulus-to-outside [kW]	27,75	23,64		21,27
Energy annulus-to-outside [GJ]	431,55	367,61		330,85
Thermal recovery [%]	**49,53%**	**57,00%**		61,30% 61,20% Result from Giordano and Raymond (2019)
				1,00 Difference with calibration (the closer to 1 the better)
Advection				
K [m/s]	1,00E-08	1,30E-05		5,00E-05
i	0,015	0,008		0,015
porosity	0,05	0,35		0,35
v Darcy [m/s]	1,50E-10	1,04E-07		7,50E-07
GW linear v	3,00E-09	2,97E-07		2,14E-06
L (6 months) [m]	0,00	1,62		11,66
Cw [MJ/m3/K]	4,2	4,2		4,2
Cg [MJ/m3/K]	2,3	2,7		3
R_{therm}	10,95	1,84		2,04
v therm [m/s]	1,37E-11	5,66E-08		3,675E-07
L_{therm} (6 months) [m]	0,00021	0,88059		5,71536
Conduction + Advection				
Convection loss [GJ]	0,01	21,23		137,80
total loss [GJ]	431,55	388,84		468,65 11,0% Result from Giordano and Raymond (2019)
Thermal recovery [%]	**49,53%**	**54,52%**		45,19% 50,30%
				0,90 Difference with calibration (the closer to 1 the better)